

Boiling Heat Transfer during Impingement of Two or Three Pipe Laminar Jets onto Moving Steel Sheet

Hitoshi FUJIMOTO,* Naoya HAYASHI, Junya NAKAHARA, Kenta MORISAWA, Takayuki HAMA and Hirohiko TAKUDA

Graduate School of Energy Science, Kyoto University, Yoshida-honmachi, Sakyo-ku, Kyoto, 606-8501 Japan.

(Received on May 17, 2016; accepted on July 4, 2016)

The impingement of pipe laminar jets is commonly used in run-out-table cooling in hot rolling mills. In this process, a moving hot steel sheet is cooled by pipe laminar array jets. When the spacing between two neighbor jets is small in the sheet width direction, flow interaction of cooling water on the sheet is inevitable, resulting in complex heat transfer phenomena. In the present study, the boiling heat transfer during the impingement of two or three pipe laminar jets onto a moving steel sheet was studied by laboratory-scale experiments. The test coolant was water at room temperature. Water jets were produced from 5-mm-diameter pipe nozzles at a mean velocity of 0.8 m/s. The nozzle spacing between two jet centers was 8, 12, or 16 mm. A 0.3-mm-thick stainless steel sheet with a moving velocity of 1.5 m/s was used as the test substrate. The temperature of steel ranged from 300 to 500°C. The flow was observed by flash photography, and the heat transfer characteristics were studied by an infrared thermography technique. It was found that high heat flux regions were formed near the jet impact points on the moving solid. Flow interaction occurred between two jets, where the heat removal rate was relatively small compared to that in the jet impact regions. The effects of the nozzle spacing, number of nozzles, and temperature of the solid on the boiling heat transfer characteristics were studied in detail from an industrial viewpoint.

KEY WORDS: run-out-table cooling; multiple-jet impingement; nozzle spacing; boiling heat transfer; flow visualization.

1. Introduction

Run-out-table (ROT) cooling in hot rolling mills is one of the key components of the thermomechanical control process.¹⁾ In ROT cooling, the desired material structures are manufactured by the rapid cooling of hot steel plates from approximately 900°C to a predetermined coiling temperature using water jet impingement. **Figure 1** shows a schematic of the temperature history of a hot steel plate during water jet cooling.²⁾ Initially, the temperature of the solid is far above the boiling temperature of the liquid. The steel is cooled softly at high temperatures of the solid because a stable vapor layer is formed between the water and steel. Such a boiling mode is called film boiling. As the cooling proceeds, the vapor film becomes thin and unstable. Direct contact between the water and solid occurs locally as well as temporally; that is, transition boiling occurs in the range between the points called the minimum heat flux (MHF) and critical heat flux (CHF). The boiling mode soon shifts to strong nucleate boiling where numerous vapor bubbles are generated at the liquid/solid interface instead of the vapor film. The heat removal rate is very large in the transition or strong nucleate boiling regime. Thereafter, the temperature variation of the solid reduces because the boiling becomes

weak.

In ROT cooling, when the coiling temperature of the solid is present in the transition or strong nucleate boiling regime, precise temperature control of the solid is difficult because of a large temperature variation of the solid. Accurate heat transfer data in these boiling regimes are required to satisfy engineering demands. Many experimental works have been undertaken concerning the boiling heat transfer involving impinging water jets.^{3,4)} Many of these studies were conducted considering single-jet impingement onto a stationary solid. However, in actual ROT cooling, pipe laminar array jets impact onto a moving hot steel plate. It is considered that the moving hot solid and the flow interaction due to

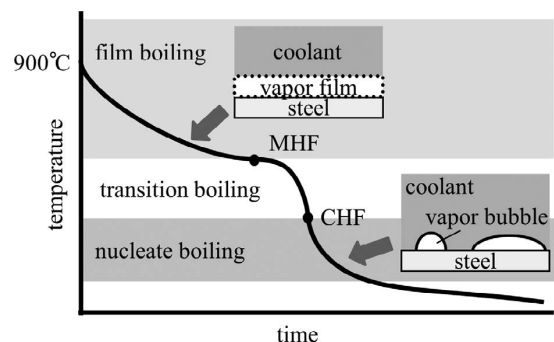


Fig. 1. Schematic of cooling curve of hot steel by water jet impingement.

* Corresponding author: E-mail: hitoshi.fujimoto.3x@kyoto-u.ac.jp
DOI: <http://dx.doi.org/10.2355/isijinternational.ISIJINT-2016-295>

multiple-jet impingement produce complicated hydrodynamic behavior of water and heat transfer characteristics. However, these factors cannot be analyzed by performing experiments involving single-jet impingement onto a stationary solid.

Some studies have analyzed single-jet impingement onto a moving hot solid.⁵⁻⁷ In addition, Ishigai *et al.*,⁸ Sakhuja *et al.*,⁹ Monde *et al.*,¹⁰ and Haraguchi and Hariki¹¹ examined multiple pipe laminar jets impinging onto a stationary hot steel plate. Recently, Vakili and Gadala¹² investigated boiling heat transfer on a hot moving plate, caused by multiple impinging water jets in rows. They found that the moving velocity of steel sheets, the spacing of nozzles, and the number of jets had some influence on the heat transfer rates in jet impingement zones. However, fundamental knowledge of the hydrodynamics of a coolant and heat transfer characteristics in such a situation is lacking. The motivation of the present study was to resolve these issues by means of laboratory-scale experiments.

The objective of the present study was to investigate the heat transfer characteristics of multiple pipe laminar water jets impinging onto a moving hot steel sheet by means of laboratory-scale experiments. Two or three identical jets were arranged in a line in the width direction of the moving sheet. The spacing between jets and the temperature of the solid were considered as the main parameters and were systematically varied. The initial temperature of the solid was varied from 300 to 500°C.

In the experiments, the flow structure of the coolant was observed by flash photography and the temperature profile of the moving solid was measured by infrared thermography.^{13,14} The heat transfer characteristics were evaluated by solving an inverse heat conduction problem by a finite volume method, using the measured temperature profile as boundary conditions. The effects of the aforementioned parameters on the hydrodynamics and heat transfer process were discussed in detail from different engineering perspectives.

2. Experimental Procedure

Figure 2 shows a schematic diagram of the experimental apparatus. Because the experimental setup was very similar to that used in our previous studies^{13,14} except for the arrangement of pipe nozzles and their auxiliary pipelines, the setup is briefly explained here. Two or three identical pipe nozzles with an inner diameter $D = 5$ mm and a pipe length of 500 mm were manufactured. The nozzles were aligned in a straight line at regular intervals in the direction of the plate width. Distilled water at approximately 17°C was used as the test coolant. Circular jets were produced vertically downward from the pipe nozzles at a mean velocity of $V_0 = 0.8$ m/s. The nozzle-to-plate spacing, H , was set 40 mm. The spacing between two successive nozzle centers, d_n , was set to 8, 12, or 16 mm.

A 60-mm-wide, 220-mm-long, and 0.3-mm-thick stainless steel (SUS430) sheet was used as the test sheet. It was firmly mounted on a linear motor actuator through thermal insulators. The underside of the sheet was coated with a thin layer of black body paint with an emissivity of $\varepsilon = 0.94$ to ensure the accurate measurement of temperature by infrared

thermography. A K-type thermocouple with a wire diameter of 0.3 mm was spot-welded on the underside of the sheet to measure the local temperature and calibrate the temperature measurement obtained by infrared thermography.

The test sheet was initially placed upstream of the test section and was electrically heated to a preset temperature (300–500°C) using a DC power supply. Then, the linear motor actuator was activated to move the test sheet into the test section at a moving velocity, V_s , of 1.5 m/s. The pipe laminar jets impacted the test sheet, and water film flows spread along the sheet surface. After the film flows appeared to become stable, images of the flows were captured by flash photography using a digital camera and flashlight. In addition, an infrared camera captured the thermal images of the rear surface of the sheet at a resolution of 320×240 pixels.

To evaluate the local temperature profile as well as the heat flux on the top surface, the inverse heat conduction problem was solved numerically using the measured temperature profile on the underside. The heat conduction equation inside the sheet in the three-dimensional Cartesian coordinate system is given as follows, assuming that the temperature profile, T , is steady in the coordinate system fixed in space:

$$\rho_p c_p V_s \frac{\partial T}{\partial x} = \lambda_p \left(\frac{\partial^2 T}{\partial x^2} + \frac{\partial^2 T}{\partial y^2} + \frac{\partial^2 T}{\partial z^2} \right), \dots \dots \dots (1)$$

where ρ_p , c_p , and λ_p represent the material properties of stainless steel (SUS430) and V_s denotes the moving velocity of the sheet. The coordinates (x, y, z) are taken in the directions of the length (x), width (y), and thickness (z). The temperature dependence of the thermophysical properties of

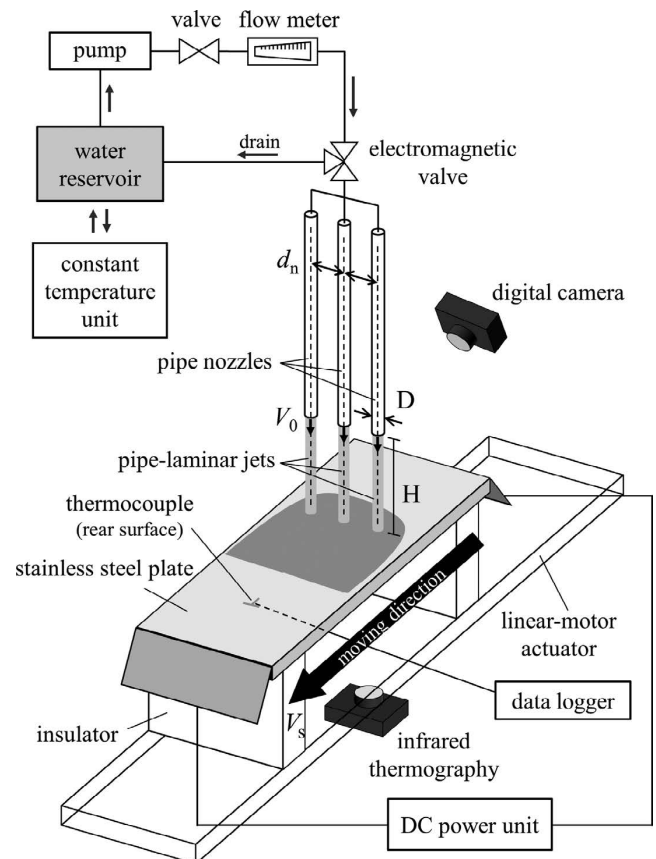


Fig. 2. Schematic of experimental apparatus.

stainless steel is taken into account. More information on the data reduction method and experimental method is available in our previous papers.^{13,14)}

3. Results and Discussion

3.1. Results for Two-jet Impingement

First, two-jet impingement was studied to understand the basic hydrodynamics and heat transfer characteristics involved in the flow interaction phenomena between jets. **Figure 3** shows photographs of the film flows formed by the impingement of two water jets. The initial temperature of the solid, T_s , is varied as 300, 400, and 500°C. The nozzle spacing, d_n , is set to 12 and 16 mm. A pair of thin water films is formed and spreads along the solid surface around the jet impact points. The flow is roughly line-symmetrical with respect to the centerline between the two jets. As expected, the width of the liquid film is larger for the larger nozzle spacing. In all the cases, liquid swelling appears at the centerline because of flow interaction. For convenience, the liquid swelling is hereafter called the vertical liquid film.

At $T_s = 300^\circ\text{C}$, strong nucleate boiling is seen. Because the flashlight is scattered by many boiling vapor bubbles and numerous minute droplets formed by bubble bursting on the free liquid surface, the water film on the solid looks cloudy. The region covered by the water film at this temperature is smaller than those at $T_s = 400$ and 500°C because boiling vapor bubbles adhering to the solid produce a large resisting force to radially spreading water. In addition, some viscous wall friction force occurs between the liquid and solid because of the local direct contact between the liquid and solid. At 400 and 500°C , the water film is transparent. Vapor films instead of bubbles are probably formed on the solid surface. The liquid films at these temperatures spread more widely than that at 300°C .

Figure 4 shows the thermal images on the rear surface under various experimental conditions. The black spot in each image represents the center point between two jet impact points. The initial steel temperature, T_s , is varied from 300 to 500°C , and the distance between two nozzles,

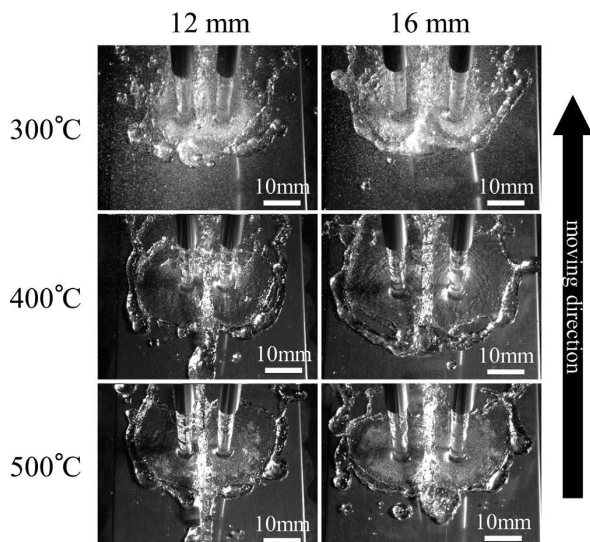


Fig. 3. Water film flow formed by impingement of two circular jets.

d_n , is chosen as 8, 12, and 16 mm. The range of the color key is 180°C in each image. For example, in the case of $T_s = 400^\circ\text{C}$, the color key ranges from 220 to 400°C . A pair of low-temperature zones elongated in the moving direction is formed in all the cases. The temperature reduction is large for $T_s = 300$ and 350°C and small for higher temperatures. In addition, relatively high-temperature areas are present in between a pair of cooling zones. These areas correspond to the vertical water film regions shown in Fig. 3. This means that the vertical liquid film has only minor influence on the cooling of test sheets.

The measured temperature profile on the rear surface is not the same as that on the cooled (wet) surface. When temperature reduction occurs in the jet impact regions, the reduction reflects on the rear surface with a certain time delay because of heat conduction. During the delay, the steel sheet travels some distance. Consequently, the temperature reduction appears not beneath the jet impact points but in the downstream region on the rear surface. Therefore, inverse heat conduction analysis is needed in the present study.

Figure 5 shows the heat flux distributions on the cooled surface estimated by the inverse heat conduction analysis. The experimental conditions are the same as those considered in Fig. 4. In addition, the range of the color key is the same in all the cases. Heat flux profiles are roughly line-symmetrical with respect to the centerline between the two jets. A pair of high heat flux regions is seen in the jet impact regions, and a relatively low heat flux region is present in between this pair. At $T_s = 300$ and 350°C , the heat flux in the jet impact regions is high owing to strong nucleate boiling. At $T_s = 450$ and 500°C , the heat flux is smaller than that at $T_s = 300$ and 350°C because the vapor bubbles/films with small thermal conductivity prevent direct contact between the water and solid. At $T_s = 450^\circ\text{C}$, the area of the high heat flux regions is smaller than that at $T_s = 400$ and 500°C , suggesting that the former temperature is close to the MHF point (see also Fig. 1). In addition, the nozzle spacing, d_n , influences the shape of the high heat flux areas in the jet impact regions. The size of these areas in the width direction is reduced as the nozzle spacing decreases, indicating that the total amount of heat removal depends on d_n .

3.2. Results for Three-jet Impingement

Figure 6 shows the photographed flow fields under the conditions $T_s = 500^\circ\text{C}$ and $d_n = 8, 12,$ and 16 mm. Three flow regions—two side flow regions and one center flow region—are divided by two vertical water films formed between two successive jets. In the side flow regions, the film flow is confined by one vertical film on one side and can spread widely on the other side. The flow structure is very similar to that for two-jet impingement. The center flow is confined by a pair of vertical liquid films on both the sides and cannot spread in the width direction. Consequently, the width of the center film flow is apparently smaller than those of the side flows. In addition, the width in the center flow region decreases as the nozzle spacing decreases.

Figure 7 shows the thermal images on the rear surface of the solid for different temperatures of the solid (300 – 500°C) and nozzle spacing ($d_n = 8, 12,$ and 16 mm). The black spot in each image represents the impact point of the center jet.

In all the cases, three low-temperature areas elongated in the moving direction are present. The local temperature reduction in the test sheet is large at $T_s = 300$ and 350°C and small at higher temperatures. The effects of the temperature of the solid on the temperature profile in the case of three-jet impingement are similar to that in the case of two-jet impingement (Fig. 4).

Two relatively high-temperature areas are seen in between the two successive low-temperature areas. These

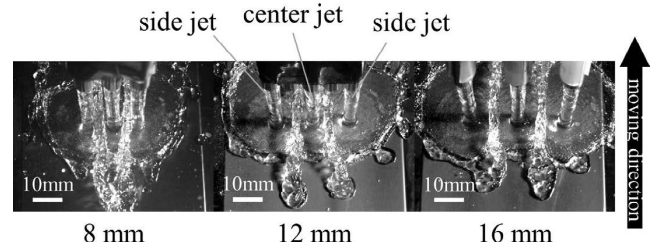


Fig. 6. Water film flow formed by impingement of three jets for $T_s = 500^\circ\text{C}$ and $d_n = 8, 12,$ and 16 mm.

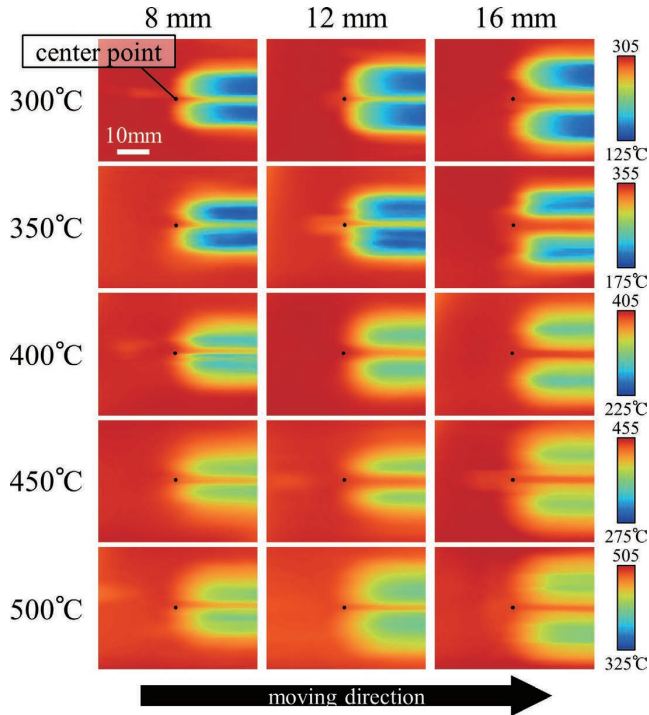


Fig. 4. Measured temperature profiles on rear surface of solid for two-jet impingement under various conditions.

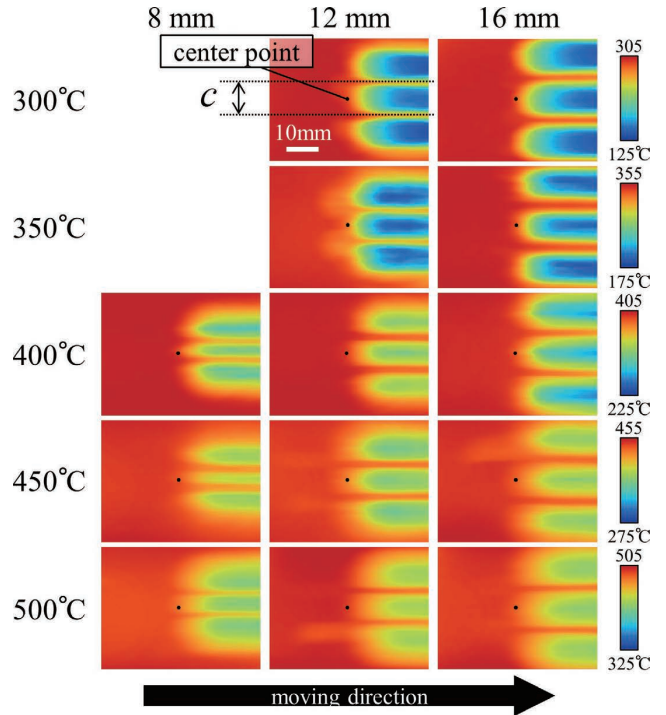


Fig. 7. Measured temperature profiles on rear surface of solid for three-jet impingement.

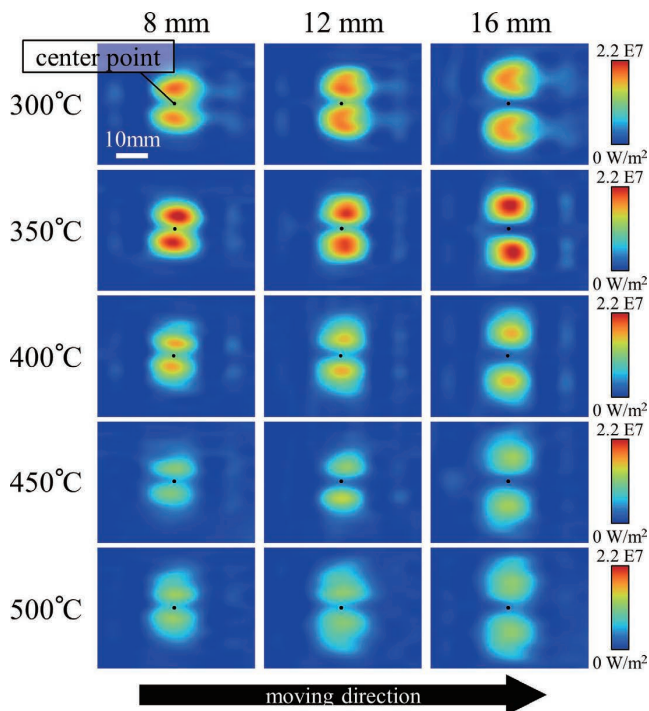


Fig. 5. Heat flux distributions for two-jet impingement calculated by performing inverse heat conduction analysis.

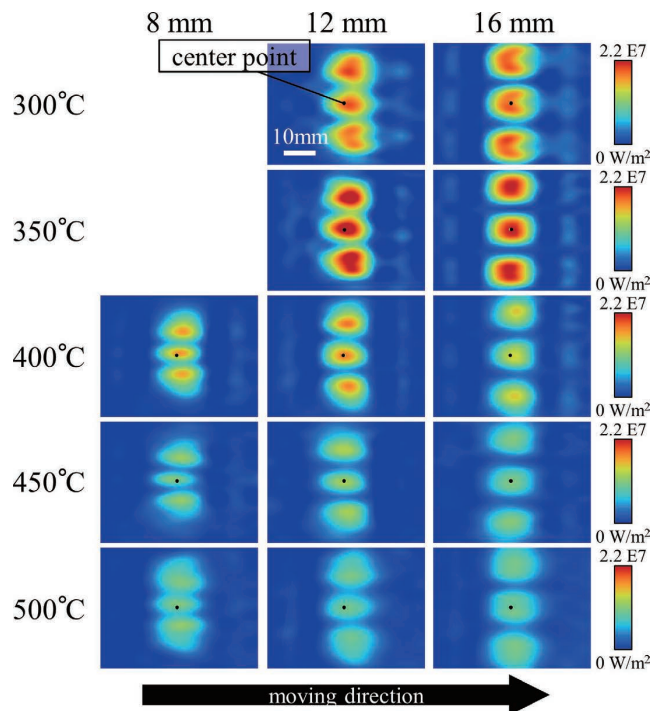


Fig. 8. Calculated heat flux distributions for three-jet impingement.

high-temperature areas coincide with the region of the vertical water films. The width of the cooling zone, C , attributable to the center jet is defined as shown in Fig. 7. This width is roughly the same as the nozzle spacing. For $d_n = 8$ mm and $T_s = 400$ – 500°C , the width of the cooling zone attributable to the center jet is distinctly smaller than those of the two side jet regions.

The experiments for $d_n = 8$ mm and $T_s = 300$ or 350°C were unsuccessful. As large temperature variations occur inside the solid during jet impingement, the resultant local thermal stress occasionally causes unwanted local buckling of the sheet. This effect is frequently observed when a large heat removal rate is imposed. As shown in the results for two-jet impingement for $d_n = 8$ mm and $T_s = 300$ or 350°C in Fig. 4, very large temperature variations are seen in the jet impact regions. In the case of three-jet impingement, very large local thermal stress is induced, resulting in unwanted local buckling of the sheet.

In our previous work,¹⁴⁾ the heat transfer characteristics of single-jet impingement were studied by varying the jet velocity, initial temperature of the solid, and velocity of the moving sheet. It was found that the heat removal rate increased as the water flow rate increased and/or the sheet velocity decreased. In the present work, we scheduled experiments for multiple-jet impingement under conditions similar to those used in the previous work. However, the experiments failed because local buckling of the sheet occurred much more frequently than in the cases of single-jet impingement. Consequently, the jet velocity was fixed to 0.8 m/s and the sheet velocity was set to 1.5 m/s in the present study.

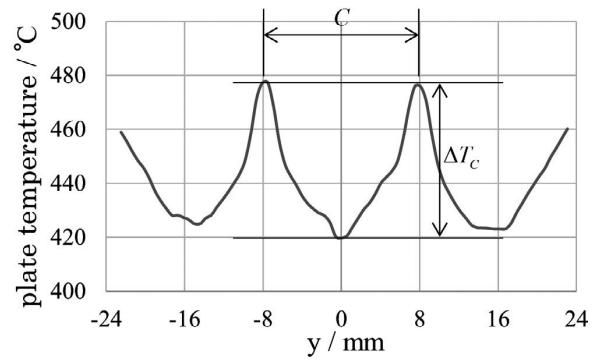
Figure 8 shows the distributions of the local heat flux on the cooled surface. The experimental conditions are the same as those considered in Fig. 7. Three high heat flux regions are observed in each heat flux profile. The maximum heat fluxes in each region are roughly comparable, but the shapes of the high heat flux regions are different. The heat flux profiles in the side flow regions are similar to those for two-jet impingement (Fig. 5). In the center flow region, the high heat flux area is reduced in the width direction. This trend is more apparent for a small nozzle spacing.

3.3. Heat Transfer Characteristics in Center Flow Region for Three-jet Impingement

In actual ROT cooling, pipe laminar jets are aligned in a straight line in the width direction. The flow formed by the impingement of each jet is confined by two neighboring jets on both the sides. Such a confined flow does not form in two-jet impingement but forms in the center flow region in three-jet impingement. From an industrial viewpoint, the heat transfer characteristics in the center film region are very important and are hence discussed in this subsection.

Figure 9 shows the temperature distribution on the rear surface in the width direction 20 mm downstream from the jet impact points for $T_s = 500^\circ\text{C}$ and $d_n = 8$ and 16 mm. Note that $y = 0$ mm denotes a line passing through the impact point of the center jet in the moving direction of the sheet. As expected, three valleys and two peaks are observed in the temperature profile. Here, we focus on the temperature variation in the center flow region between the two peaks, indicated by the distance C in the figure. As

(a) $d_n = 16$ mm



(b) $d_n = 8$ mm

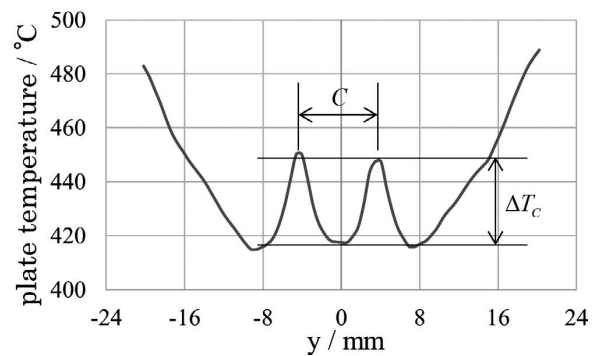


Fig. 9. Temperature distribution on rear surface 20 mm downstream of jet impact point in width direction for $T_s = 500^\circ\text{C}$.

already explained, the distance C is almost equal to the nozzle spacing. In the center region, the range of temperature variation, ΔT_c , which is defined in the figure, is distinctly smaller for a smaller C . Similar results are obtained for other temperatures of the solid. In actual ROT cooling, a uniform temperature profile of the solid in the width direction is preferable to produce high-quality steel sheets. Accordingly, a small nozzle spacing is desirable.

Next, the heat removal in the center jet region is discussed quantitatively. Because the areas having relatively high heat flux are dependent on the nozzle spacing (Fig. 8), the following equation is introduced:

$$Q_C = \int_S q dS \quad S: -\frac{1}{2}d_n \leq y \leq \frac{1}{2}d_n \text{ and } q \geq q_{\text{threshold}} \dots (2)$$

Here, Q_C is a total heat removal amount calculated by the integration of the local heat flux, q , in the jet impact region, S , where the local heat flux is equal to or larger than a threshold value, $q_{\text{threshold}}$, in the range $-d_n/2 \leq y \leq d_n/2$. The value $q_{\text{threshold}}$ is introduced so as to ignore small heat flux regions where small amounts of cooling water is present or thick vapor films cover the solid surface. The total heat removal amount as well as the area of S varies absolutely depending on the choice of $q_{\text{threshold}}$. These parameters increase as $q_{\text{threshold}}$ decreases. Because there is no theoretical method to determine an appropriate value of $q_{\text{threshold}}$, three values are chosen: 1×10^5 , 5×10^5 , and 1×10^6 W/m².

Figure 10 shows the total heat removal amount attributable to the center jet when $q_{\text{threshold}}$ is set to 1×10^5 W/m². The total heat removal amount Q_C is high at 300 or 350°C and sharply reduces at 400°C. In addition, Q_C decreases as

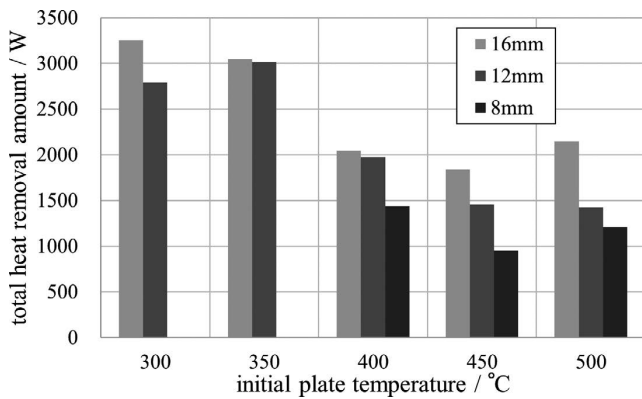


Fig. 10. Heat removal amount in center jet region calculated using Eq. (2).

the nozzle spacing decreases. This is mainly because the width of the center film flow reduces. Similar results are obtained for the other threshold values (5×10^5 and 1×10^6 W/m²).

The results in Figs. 9 and 10 indicate that employing a small nozzle spacing is useful for obtaining small temperature variations of the solid in the width direction. On the other hand, employing a small nozzle spacing leads to an increase in the number of nozzles in the cooling equipment, and consequently, the total heat removal amount per pipe laminar jet becomes small. As a result, a large amount of water is needed to achieve the desired heat reduction.

4. Conclusions

In this study, the boiling heat transfer characteristics on a hot plate cooled by multiple pipe laminar jets are investigated experimentally. The initial sheet temperature, number of jets, and distance between nozzles are varied in the experiments. The main results obtained in this study are summarized below:

(1) In the case of two-jet impingement, flow interaction is observed in the region between the two jet impact points. The formation of a vertical liquid film is one of the characteristic features of the flow interaction, but the film formation does not promote heat removal. The flow and temperature profiles of the solid are roughly line-symmetrical with respect to the centerline between the two jets. The heat flux

is strongly dependent on the temperature of the steel sheet. In addition, the nozzle spacing affects the shape of the high heat flux regions.

(2) For three-jet impingement, two types of flow regions are observed: two side jet regions and one center jet region. In the side jet regions, the flow mechanics are similar to those for two-jet impingement. In the center jet region, the flow is confined by two vertical liquid films on both the sides. The cooling width of the center jet region corresponds to the nozzle spacing. In the center jet region, the temperature variation of the solid in the width direction becomes small for a small nozzle spacing. This result suggests that moderately uniform cooling can be achieved in actual ROT cooling if a small nozzle spacing is employed. However, the total heat removal amount per pipe laminar jet reduces, and hence, the amount of cooling water required increases.

Acknowledgement

The present work has been supported by the 24th Research Promotion Grant from the Iron and Steel Institute of Japan.

REFERENCES

- 1) M. Mitsutsuka and K. Fukuda: *Tetsu-to-Hagané*, **75** (1989), 1154.
- 2) N. Hatta, J. Kokado and K. Hanasaki: *Trans. Iron Steel Inst. Jpn.*, **23** (1983), 555.
- 3) D. H. Wolf, F. P. Incropera and R. Viskanta: *Adv. Heat Transf.*, **23** (1993), 1.
- 4) J. Hammad, M. Monde and Y. Mitsutake: *Therm. Sci. Eng.*, **12** (2004), 19.
- 5) S. Chen, J. Kothari and A. Tseng: *Exp. Therm. Fluid Sci.*, **4** (1991), 343.
- 6) M. Gradeck, A. Kouachi, M. Lebouche, F. Volle, D. Maillat and J. L. Boreau: *Int. J. Heat Mass Transf.*, **52** (2009), 1094.
- 7) M. Gradeck, A. Kouachi, J. L. Boreau, P. Gardin and M. Lebouche: *Int. J. Heat Mass Transf.*, **54** (2011), 5527.
- 8) S. Ishigai, S. Nakanishi, M. Mizuno and T. Imamura: *Bull. Jpn. Soc. Mech. Eng.*, **20** (1977), 85.
- 9) R. Sakhuja, F. Lazgin and M. Oven: ASME Paper 80-HT-47, ASME, New York, (1981), 47.
- 10) M. Monde, H. Kusuda and H. Uehara: *Heat Transf. Jpn. Res.*, **9** (1982), 18.
- 11) Y. Haraguchi and M. Hariki: 2nd Int. Conf. on Modelling of Metal Rolling Processes, ed. by J. H. Beynon, Institute of Materials, London, (1996), 606.
- 12) S. Vakili and M. S. Gadala: *Heat Transf. Eng.*, **34** (2013), 580.
- 13) H. Fujimoto, K. Tatebe, T. Hama and H. Takuda: *ISIJ Int.*, **54** (2014), 1338.
- 14) H. Fujimoto, Y. Shiramasa, K. Morisawa, T. Hama and H. Takuda: *ISIJ Int.*, **55** (2015), 1994.